

## Comparative Study the Effect of Irradiation on Cobalt Complexes Before and After Irradiation

Samar A. Aly<sup>1\*</sup>, Safaa S. Hassan<sup>2</sup>, Emad F. Newair<sup>3</sup>, Ehab M. Abdalla<sup>4\*</sup>, Ayman E. Hassan<sup>1</sup>

<sup>1\*</sup> Department of Environmental Biotechnology, Genetic Engineering and Biotechnology Research Institute, University of Sadat City, 32958, Egypt.

<sup>2</sup> Chemistry Department, Faculty of Science, Cairo University, Giza 12613, Egypt.

<sup>3</sup> Chemistry Department, Faculty of Science, Sohag University, Egypt.

<sup>4\*</sup> Chemistry Department, Faculty of Science, New Valley University, Alkharga 72511, Egypt.

DOI: 10.21608/rjab.2024.307078.1053

\*Corresponding author1: Prof. Samar A. Aly

E-mail: [samar.mostafa@gebri.usc.edu.eg](mailto:samar.mostafa@gebri.usc.edu.eg)

Tel: +201063936729

\*Corresponding author2: Dr. Ehab M. Abdalla

E-mail: [Ehababdalla99@sci.nvu.edu.eg](mailto:Ehababdalla99@sci.nvu.edu.eg)

Tel: +201008275126

### ABSTRACT:

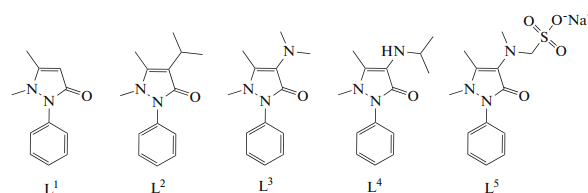
N-(1,5-dimethyl-3-oxo-2-phenyl-2,3-dihydro-1H-Pyrazol-4-yl) carbonohydranoyl dicyanide (LB) is operated to produce and describe the novel Co(II) complex (CB). The structural compositions of the new compounds were clarified through the utilization of analytical and spectroscopic techniques. This study examines the effects of gamma radiation on the Co(II) complex of the ligand and its biological activity (B and A before and after irradiation). Theoretical measurements supported the proposed generic formula for the  $[\text{CoLCl}_2 (\text{H}_2\text{O})_2]$  complex as well as the results of thermal analysis, FTIR, molar conductivity and elemental analysis, the complex produced with a molar ratio of 1:1 M:L. The antibacterial activities of the chemical were assessed using ampicillin, gentamicin as standards, and the following sequence of activities was observed: (CA) presented the highest activity, followed by  $\text{CA} > \text{CB} > \text{LA} > \text{LB}$ . The molecular docking process's objective study was to investigate the binding between the complex with Penicillin-binding protein PBP, which is responsible for supporting microbial inhibitory growth.

**Keywords:** Complex, Gamma Irradiation, antibacterial, Molecular Docking

### 1. INTRODUCTION

The substance known as antipyrine (1,5-dimethyl-2-phenylpyrazole-3-one) L1 has a pyrazolone moiety, which is a five-membered heterocyclic ring that houses a ketone group and two neighboring nitrogen groups inside the same molecule. Ludwig Knorr coined the word "antipyrine" in the late 1700s. The first synthetic analgesic drug was antipyrine. and was the drug most frequently used prior to aspirin was synthesized in the initial 1900s (Cechinel Filho *et al.*, 1998;

Cunha *et al.*, 2005). Several substances based on antipyrine, such as isopropyl antipyrine L2, aminopyrine L3, Ramifenazone L4, and Dipyrone L5, were created through strategic derivatization and are widely utilized as analgesics and anti-inflammatory



medications around the world (Brogden, 1986; Ravina, 2011).

Ampyrone, sometimes referred to as 4-Aminoantipyrine, is an antipyrine derivative with a variety of biological activities that has an amino group at position C-4 (Mohanram and Meshram, 2014). Taking advantage of the amino group's reactivity which can be advantageous while forming Schiff bases by reacting with aldehyde/keto compounds or condensing with acyl or alkyl halides.

Many variants of this system have been developed. However, the cyclic ketonic group's reactivity has also been used to couple with a variety of amine derivatives to produce compounds with fascinating ligational behavior. Furthermore, these compounds have formed flexible transition metal complexes by acting as ligands. That may have medical applications, including those related to oxidative dismutase (Joseph *et al.*, 2015), insulin-producing (Umadevi *et al.*, 2019), and so on (Khalaf-Alla, 2020; Abdalla *et al.*, 2021; Aly *et al.*, 2022). Moreover, Cobalt(II) complexes are widely recognized for their potent antibacterial, antiproliferative, nuclease, anti-inflammatory, and antimycobacterial characteristics (Turomsha *et al.*, 2022). The synthesis, characterization, and bioactivities of a cobalt complex with a ligand derived from antipyrine derivatives are discussed below, along with the impact of gamma irradiation.

## 2. MATERIAL AND METHODES

Comprehensive details regarding the supplies, apparatuses, and methods utilized in relation to structural validation and proposal can be found in the supplemental file (Section S1). (Section S2): antimicrobial treatment (Hare, 1968; Abdalla *et al.*, 2020; Aly *et al.*, 2023).

### 2.1. Synthesis of Compound

The metal complex was prepared by stirring magnetically at 60 °C for the solution of 0.002 moles of  $\text{CoCl}_2 \cdot 2\text{H}_2\text{O}$  in ethanol with the 0.002 moles of the appropriate ligands in 50 ml EtOH for periods 4-6 hr

(Abdalla and Abd-Allah, 2022; Abo-Rehab *et al.*, 2024). The resultant particles were removed by filtering, repeatedly cleaned with EtOH, and vacuum-dried over  $\text{P}_4\text{O}_{10}$  (Structures 1).

## 3. RESULTS AND DISCUSSION

### 3.1. Properties of the Compounds

#### 3.1.1. Physicochemical properties

When exposed to air and moisture, Co (II) complex maintains its hue. The complex's analytical results validate the creation of 1:1 (M:L) complex, (Table,1) & structures 1, and are consistent with the molecular formulas proposed. The molar conductivity value of  $C_B$  is  $33 \Omega^{-1}\text{cm}^2\text{mol}^{-1}$  in DMF solution. Their non-electrolytic nature is shown by the values of complex (Nunes *et al.*, 2020; Sardaru *et al.*, 2021).

### 3.2. FT-IR spectra of Compounds

Four bands are identified in the ligand at 3201, 2206, 1635, and 1589  $\text{cm}^{-1}$  in the infrared spectrum (Table 2 and Figure 1) as  $\nu$  (N-H),  $\nu$  (C=N),  $\nu$  (C=O), and  $\nu$  (C=N), respectively.

#### 3.2.1. FT-IR spectra of cobalt (II) complexes ( $C_B$ and $C_A$ ) before and after $\gamma$ -irradiation

Strong bands at 3441, 3191, 2175, 1600, 1604, 555, 594 and 450 and 476  $\text{cm}^{-1}$  are ascribed to  $\nu$ (OH)/ $\text{H}_2\text{O}$ ,  $\nu$ (N-H),  $\nu$  (C=N),  $\nu$  (C=O) and  $\nu$  (C=N),  $\nu$  (M-O) and  $\nu$  (M-N) correspondingly in the IR spectra of  $C_B$  and  $C_A$  complexes (Table 2 and Figure 2) prior to irradiation. Following gamma irradiation, these bands move to a higher frequency of the function group band (Aly *et al.*, 2021).

### 3.3. Electronic spectra

The UV-Vis spectra of the ligand and Co (II) complex were obtained in DMSO at room temperature, at the wavelength range of 200–800 nm. There are two absorption bands visible in the ligand's absorption spectra. The initial high intensity band seen at  $\lambda_{\text{max}} = 0.0000266 \text{ cm}$  may be caused by the aromatic rings'  $\pi \rightarrow \pi^*$  transition. The second bands at

0.0000378 cm are caused by charge transfer and the  $n \rightarrow \pi^*$  transition of the azomethine group (C=N). The electronic spectra of the complex demonstrated that the azomethine nitrogen was coordinated to the metal ions, as evidenced by bands that were displaced to 0.0000275 and 0.0000389 cm for the  $\pi-\pi^*$  and  $n-\pi^*$  transitions, respectively, when compared to those of the free ligand (Mishra *et al.*, 2016; Ribeiro *et al.*, 2017).

### 3.4. ESI-MS spectra

The mass spectra of  $C_B$  complex show molecular peaks at 447.17 amu. The hypothesized chemical formulae for Co (II) complexes agree well with these findings (Figure 3).

### 3.5. X-ray diffraction

Since the single crystal development was unsuccessful, all compounds underwent powder X-ray diffraction (PXRD) analysis. Figure 4 shows the PXRD of the ligand and Co (II) combination over  $2\theta = 5-80^\circ$ .  $L_B$  and  $C_B$  complex's well-defined crystalline peaks were visible in the patterns. Using the Scherer equation (Muniz *et al.*, 2016; Abdel-Rahman *et al.*, 2021), the average particle sizes of the ( $L_B$  and  $C_B$ ) complex were determined to be 27.52 and 29.21, respectively. Scanning electron microscopy (SEM) was used to examine the surface morphology of Co chelates, as shown in Figures 5 and 6, in order to make the spherical shape of each chelate more evident. Every chelate was effectively synthesized at the nanoscale.

### 3.6. Thermogravimetric analysis

The behavior of the thermals was investigated using thermogravimetric techniques of the compounds combination during a temperature range of 25 to 800 °C. The outcomes are displayed in Table 3. The total gel time (TG) of the ligand was shown to be partially decomposed at temperatures between 98 and 425 °C, and fully decomposed at temperatures over 425 °C. Three weight-loss events are visible on the

Co (II) complex's TG curves. The loss of two hydrated  $H_2O$  and one coordinated  $H_2O$  occurs during the first breakdown stage, which occurs between 25 and 200 °C, this is read as a weight loss of (Found/Calc. %); 8.35 (8.39). The breakdown of the  $C_{17}H_{10}Cl_2N_2OS$  moiety takes place in the second step, which is between 200 and 398 °C, the anticipated weight loss range for this phase is (Found/Calc. %; 56.25 (56.18)). The projected mass reduction for the third stage, which occurs between 398 and 600 °C, is 22.97 (23.06) (Found/Calc.%), is thought to represent the full breakdown of the  $C_7H_4N_2S$  moiety, leaving CoO as the final residue.

### 3.7. DFT Calculation:

Using the Gaussian 09 program (Frisch *et al.*, 1988) at B3LYP/6-311G+(dp) for all atoms except metal ions at B3LYP/LANL2DZ level of theory for the ligands and their complexes, Density Functional Theory (DFT) calculations have been performed to study the equilibrium geometry of the ligand and  $[CoLCl_2(H_2O)_2]$ .

#### - Molecular DFT Calculation of $[CoLCl_2(H_2O)_2]$ :

Figure 7, shows the optimized structures of the complex  $[CoLCl_2(H_2O)_2]$  as the lowest energy configurations. The cobalt atom is six-coordinated in an octahedral geometry, where the dihedral angle is  $0.749^\circ$  for atoms O1, N4, O3 and Cl2, Table 4.

The distance between N4- - -O1 in the ligand (4.153 Å) is lowered in the complex are 2.897 Å due to complex formation.

The natural charges computed from the NBO-analysis on the coordinated atoms are Co (+1.358), O1 (-0.466), O2 (-0.479), O3 (-0.469), Cl<sub>1</sub> (-0.563), Cl<sub>2</sub> (-0.653) and N<sub>4</sub> (-0.563).

Table 5 computes the dipole moment, the highest and lowest occupied molecular orbital (HOMO) and LUMO energies, as well as the computed total energy for the ligands and complexes. The complexes are more stable than the free ligands, as indicated by the more negative values of the complexes' total energies compared to the

free ligand. Moreover, the Co(II) complex exhibits smaller energy gaps (Eg = ELUMO - EHOMO) than the ligand due to ligand chelation to metal ions (Table 1). The charge transfer interactions during complex formation are explained by the reduction in Eg in the complex relative to the ligand (Figure 8). The complex appear to be more reactive than the ligand, as indicated by their smaller hardness and larger softness. Soft molecules are more reactive than hard molecules and are more susceptible to variations in electron density. Because the complexes' dipole moments are smaller than the ligand's, the complexes' reduced polarity is caused by the ligand's partial sharing of the donor group's positive charge with the metal ion.

### 3.8. Antibacterial bioassay

It has been discovered that some pharmaceutical medications are more efficient against Gram-positive bacteria than Gram-negative bacteria. In this investigation, the antibacterial activity of the L<sub>B</sub> and C<sub>B</sub> complex was assessed using the agar diffusion technique against Gram-ve bacteria *P. vulgaris* and *E. coli* as well as Gram +ve bacteria *S. aureus* and *B. subtili*. Table 6 and Figure 9 present a list of the measured bactericidal activity of Co (II) and ligand (Reedijk and Bouwman, 1999). When the ligand chelated with Co (II) to form complexes, we saw an increase in the ligand's activity against several bacterial strains. The partial sharing of the metal ion's positive charge with the donor (N and O) atoms of the ligand, which results in electron delocalization throughout the entire chelate ring system, accounts for the complexes' increased antibacterial activity. Considering that the complex's geometrical shape, the kind of donor atoms, the metal ion, the complex ion's overall charge and the ligands' chelating action all influence the biological activity of metal compounds (Ispir, 2009). The cobalt complex exhibits potent antibacterial effect against the investigated microorganisms especially *E. coli* and *B. cereus*. In order to support the microbial

inhibition of growth, a molecular docking study was conducted to investigate the binding between the complex and Penicillin-binding protein PBP. PBP is primarily thought of as a precursor for the biosynthesis of cell walls through transglycosylation and transpeptidation. Replacement in PBP can result in the production of pathogenic bacteria strains that are resistant to antibiotics. The mutant-type PBP5 structure (PDB ID: 1NJ4) was retrieved from the Protein Data Bank. Figure 10 displays the complex's interaction analyses. The interaction was performed with scoring energy value -9.00 kcal/mol. The active amino acids are Met 89 and Asp 105 that show interactions of Metal Contact and Sidechain acceptor, respectively (Pisano *et al.*, 2019; El-Etrawy and Sherbiny, 2021).

## 4. CONCLUSION

This work used a variety of spectroscopic and structural methods to completely describe and create novel Co (II) complex. They assessed their biological activity against several bacterial strains. It was discovered that Co (II) complex exhibited greater efficacy against distinct strains of bacteria than it did against ligand. According to the results of thermal analysis, FTIR, molar conductivity and elemental analysis, the complex produced with a molar ratio of 1:1 M:L and the formula [CoLCl<sub>2</sub> (H<sub>2</sub>O)<sub>2</sub>].

## 5. REFERENCES

- Abdalla, E.M., and Abd-Allah, M. (2022). Synthesis, Characterization, Antimicrobial/Antitumor Activity of Binary and Ternary Neodymium (III) Complex with 2, 2'-((1E, 1'E)-(ethane-1, 2-diylbis (azaneylylidene)) bis (methaneylylidene)) diphenol and Imidazole. *Egyptian Journal of Chemistry* 65, 735-744.
- Abdalla, E.M., Abdel Rahman, L.H., Abdelhamid, A.A., Shehata, M.R., Alothman, A.A., and Nafady, A. (2020). Synthesis, characterization, theoretical studies, and antimicrobial/antitumor potencies of salen and salen/imidazole complexes of Co (II), Ni (II), Cu (II), Cd (II), Al (III) and La (III). *Appl. Organomet. Chem.* 34, e5912.

- Abdalla, E.M., Hassan, S.S., Elganzory, H.H., Aly, S.A., and Alshater, H. (2021). Molecular docking, DFT calculations, effect of high energetic ionizing radiation, and biological evaluation of some novel metal (II) heteroleptic complexes bearing the thiosemicarbazone ligand. *Molecules* 26, 5851.
- Abdel-Rahman, L.H., Basha, M.T., Al-Farhan, B.S., Shehata, M.R., and Abdalla, E.M. (2021). Synthesis, characterization, potential antimicrobial, antioxidant, anticancer, DNA binding, and molecular docking activities and DFT on novel Co (II), Ni (II), VO (II), Cr (III), and La (III) Schiff base complexes. *Applied Organometallic Chemistry* 36, e6484.
- Abo-Rehab, R.S., Kasim, E.A., Farhan, N., Tolba, M.S., Shehata, M.R., and Abdalla, E.M. (2024). Synthesis, characterization, anticancer, antibacterial, antioxidant, DFT, and molecular docking of novel La (III), Ce (III), Nd (III), and Dy (III) lanthanide complexes with Schiff base derived from 2-aminobenzothiazole and coumarin. *Applied Organometallic Chemistry*, e7622.
- Aly, S.A., Eldourghamy, A., El-Fiky, B.A., Megahed, A.A., El-Sayed, W.A., Abdalla, E.M., and Elganzory, H.H. (2023). Synthesis, spectroscopic characterization, thermal studies, and molecular docking of novel Cr (III), Fe (III), and Co (II) complexes based on Schiff base: In vitro antibacterial and antitumor activities. *Journal of Applied Pharmaceutical Science* 13, 196-210.
- Aly, S.A., Elganzory, H.H., Mahross, M.H., and Abdalla, E.M. (2021). Quantum chemical studies and effect of gamma irradiation on the spectral, thermal, X-ray diffraction and DNA interaction with Pd (II), Cu (I), and Cd (II) of hydrazone derivatives. *Appl. Organomet. Chem.* 35, e6153.
- Aly, S.A., Hassan, S.S., Eldourghamy, A.S., Badr, E.E., El-Salamoney, M.A., Hassan, M.A., and Elganzory, H.H. (2022). Synthesis, characterization, XRD, SEM, DNA binding, and effect of  $\gamma$ -irradiation of some new Ni (II) and Co (II) complexes with thiosemicarbazone ligand: in vitro antimicrobial and antioxidant activities. *Applied Organometallic Chemistry* 36, e6727.
- Brogden, R.N. (1986). Pyrazolone derivatives. *Drugs* 32, 60-70.
- Cechinel Filho, V., Corrêa, R., Vaz, Z., Calixto, J.B., Nunes, R.J., Pinheiro, T.R., Andricopulo, A.D., and Yunes, R.A. (1998). Further studies on analgesic activity of cyclic imides. *Il Farmaco* 53, 55-57.
- Cunha, S., Oliveira, S.M., Rodrigues Jr, M.T., Bastos, R.M., Ferrari, J., De Oliveira, C.M., Kato, L., Napolitano, H.B., Vencato, I., and Lariucci, C. (2005). Structural studies of 4-aminoantipyrine derivatives. *Journal of Molecular Structure* 752, 32-39.
- El-Etrawy, A.-a.S., and Sherbiny, F.F. (2021). Design, synthesis, biological assessment and molecular docking studies of some new 2-Thioxo-2, 3-dihydropyrimidin-4 (1H)-ones as potential anticancer and antibacterial agents. *Journal of Molecular Structure* 1225, 129014.
- Frisch, M., Trucks, G., Schlegel, H., Scuseria, G., Robb, M., Cheeseman, J., Scalmani, G., Barone, V., Mennucci, B., and Petersson, G. (1988). Gaussian 09, revision A. 02, Gaussian, Inc., Wallingford, CT, 2009 Search PubMed;(b) C. Lee, W. Yang and RG Parr. *Phys. Rev. B: Condens. Matter Mater. Phys.* 37, 785.
- Hare, C.R. (1968). *Visible and Ultra Violet Spectroscopy*. John Wiley and Sons. New York, USA: John Wiley and Sons.
- Ispir, E. (2009). The synthesis, characterization, electrochemical character, catalytic and antimicrobial activity of novel, azo-containing Schiff bases and their metal complexes. *Dyes and Pigments* 82, 13-19.
- Joseph, A.A., Joseph, A., and Abizari, A. (2015). Effects of varied parboiling conditions on proximate and mineral composition of Jasmine-85 and Nerica-14 rice varieties in Ghana. *International journal of food research* 2, 1-11.
- Khalaf-Alla, P.A. (2020). antioxidant, antimicrobial and antitumor studies of transition metal complexes derived from N-(2-Aminoethyl)-1, 3-propanediamine with DFT calculations and molecular docking investigation. *Applied Organometallic Chemistry* 34, e5628.
- Mishra, N., Poonia, K., Soni, S.K., and Kumar, D. (2016). Synthesis, characterization and antimicrobial activity of Schiff base Ce (III) complexes. *Polyhedron* 120, 60-68.
- Mohanram, I., and Meshram, J. (2014). Synthesis and Biological Activities of 4-Aminoantipyrine Derivatives Derived from Betti-Type Reaction. *International Scholarly Research Notices* 2014, 639392.
- Muniz, F.T.L., Miranda, M.a.R., Morilla Dos Santos, C., and Sasaki, J.M. (2016). The Scherrer equation and the dynamical theory of

- X-ray diffraction. *Acta Crystallographica Section A: Foundations and Advances* 72, 385-390.
- Nunes, D.M., Pessatto, L.R., Mungo, D., Oliveira, R.J., De Campos Pinto, L.M., Da Costa Iemma, M.R., Altei, W.F., Martines, M.a.U., and Duarte, A.P. (2020). New complexes of usnate with lanthanides ions: La (III), Nd (III), Tb (III), Gd (III), synthesis, characterization, and investigation of cytotoxic properties in MCF-7 cells. *Inorganica Chim. Acta* 506, 119546.
- Pisano, M.B., Kumar, A., Medda, R., Gatto, G., Pal, R., Fais, A., Era, B., Cosentino, S., Uriarte, E., and Santana, L. (2019). Antibacterial activity and molecular docking studies of a selected series of hydroxy-3-aryl coumarins. *Molecules* 24, 2815.
- Ravina, E. (2011). *The evolution of drug discovery: from traditional medicines to modern drugs*. John Wiley & Sons.
- Reedijk, J., and Bouwman, E. (1999). *Bioinorganic catalysis*. CRC Press.
- Ribeiro, N., Roy, S., Butenko, N., Cavaco, I., Pinheiro, T., Alho, I., Marques, F., AVECILLA, F., Pessoa, J.C., and Correia, I. (2017). New Cu (II) complexes with pyrazolyl derived Schiff base ligands: synthesis and biological evaluation. *J. Inorg. Biochem.* 174, 63-75.
- Sardaru, M.-C., Marangoci, N.L., Shova, S., and Bejan, D. (2021). Novel Lanthanide (III) Complexes Derived from an Imidazole–Biphenyl–Carboxylate Ligand: Synthesis, Structure and Luminescence Properties. *Molecules* 26, 6942.
- Turomsha, I.S., Gvozdev, M.Y., Loginova, N.V., Ksendzova, G.A., and Osipovich, N.P. (2022). Synthesis, characterization and biological activity of Hydrazones and their copper (II) complexes. *Chemistry Proceedings* 12, 73.
- Umadevi, M., Muthuraj, V., and Vanajothi, R. (2019). Synthesis of coumarin derivatives and its Ru (II) complexes encompassing pyrazole ring as a potent antidiabetic agents—a biochemical perspective. *Inorganica Chimica Acta* 492, 48-59.

**Table 1.** Analytical data of the compounds.

Compounds	Color Yield %	Molecular weight	Conductivity $\mu\text{s}$	M. P. $^{\circ}\text{C}$	Found (cal.) %			
					C	H	N	M
<b>Ligand</b> $\text{C}_{14}\text{H}_{12}\text{N}_6\text{O}$	Orange 84	280.11	-	151	59.56 (59.99)	4.28 (4.32)	29.91(29.98)	-
<b>Co(II) complex</b> $\text{C}_{14}\text{H}_{16}\text{C}_{12}\text{CoN}_6\text{O}_3$	Brown 75	446.15	33	293	37.31 (37.69)	3.52 (3.61)	18.76 (18.84)	13.09 (13.21)

**Table 2.** FT-IR spectral values for Compounds.

No.	Compounds	$\nu(\text{OH})/\text{H}_2\text{O}$	$\nu(\text{N-H})$	$\nu(\text{C=N})$	$\nu(\text{C=O})$	$\nu(\text{C=N})$	$\nu(\text{M-O})$	$\nu(\text{M-N})$
	$\text{L}_B$	-	3201	2206	1635	1589	-	-
$\text{C}_B$	$\text{Co}(\text{HL})(\text{H}_2\text{O})_2\text{Cl}_2$	3441	3191	2175	1600	1550	555	450
$\text{C}_A$		3448	3200	2222	1604	1558	594	476

**Table 3.** Thermal values of the compounds

Compound	TAG(A)/ $^{\circ}\text{C}$	Wt. loss Found (Calc.) %	Leaving species
<b>Ligand</b>	98-425	83.26 (83.15)	decomposition of the partial of organic ligand
<b>Residue</b>	> 425	16.74 (16.84)	complete decomposition of the organic ligand
<b>Co(II) complex</b>	25-200	8.35 (8.39)	$2\text{H}_2\text{O}_{\text{hyd}} + \text{H}_2\text{O}_{\text{coor}}$
	200-398	56.25 (56.18)	$\text{C}_{17}\text{H}_{10}\text{Cl}_2\text{N}_2\text{OS}$
	398-600	22.97 (23.06)	$\text{C}_7\text{H}_4\text{N}_2\text{S}$
<b>Residue</b>	>600	12.42 (12.37)	<b>CoO</b>

**Table 4.** Important optimized bond lengths (Å) and bond angles (°) of [CoLCl<sub>2</sub> (H<sub>2</sub>O)<sub>2</sub>].

Type of bond	Bond length(Å) Complex	Type of bond	Bond length(Å) L Complex	
Co-N4	1.841	Co-Cl1	-	2.281
Co-O1	1.956	Co-Cl2		2.291
Co-O2	2.027	N4- - - -O1	4.153	2.897
Co-O3	1.994			
Type of Angle	Angle (°) Complex	Type of Angle	Angle (°) Complex	
N4-Co-O1	85.61	O1-Co-O2	77.77	
N4-Co-O3	91.30	O1-Co-Cl2	85.25	
N4-Co-O2	95.16	O1-Co-O3	169.26	
N4-Co-Cl1	85.61	O2-Co-Cl1	178.20	
N4-Co-Cl1	172.13	N4-Co-Cl2	172.13	
O1-Co-Cl1	100.50	Cl1-Co-Cl2	99.82	
Cl2-Co-O2	79.56	O1-N4-O3-Cl2	0.749*	
Cl2-Co-O3	84.02			

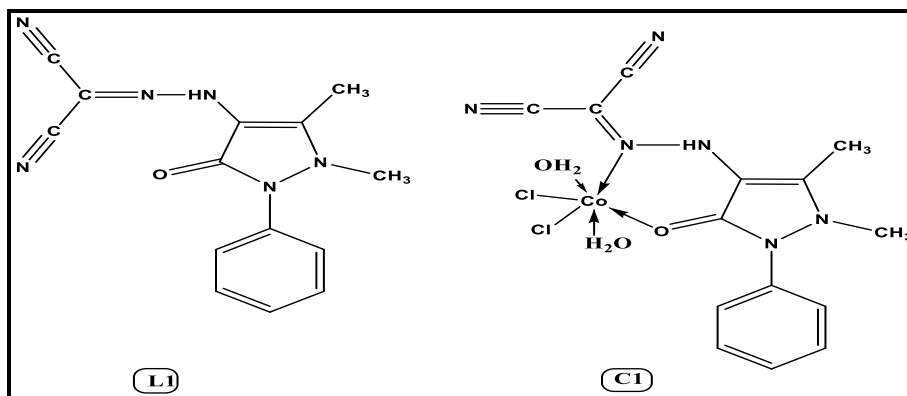
\*dihedral angle

**Table 5.** Calculated properties of [CoLCl<sub>2</sub> (H<sub>2</sub>O)<sub>2</sub>] complex.

Property	[CoLCl <sub>2</sub> (H <sub>2</sub> O) <sub>2</sub> ]
The total energy E (a.u.)	-1782.35
HOMO (eV)	-7.379
LUMO (eV)	-2.7926
E <sub>g</sub> =E <sub>LUMO</sub> - E <sub>HOMO</sub> (eV)	4.5864
Dipole moment (Debye)	10.62
ionization potential I=-E <sub>HOMO</sub>	7.379
electron affinity A=-E <sub>LUMO</sub>	2.7926
Electronegativity $\chi=(I+A)/2$	-5.0858
chemical hardness $\eta=(I -A)/2$	2.2932
chemical softness S=1/2 $\eta$	0.4360
chemical potential $\mu=-\chi$	5.0858
Electrophilicity $\omega=\mu^2/2\eta$	5.6395

**Table 6.** The *in-vitro* antibacterial activity:

	B. cereus	Staph. Aureus	E. coli	E. cloacae	B. cereus	Staph. Aureus	E. coli	E. cloacae
<b>Ligand (HL<sub>B</sub>)</b>	15.6	62.5	7.81	62.5	62.5	250	31.3	125
<b>Co(II) complex (CB)</b>	31.3	125	15.6	125	125	500	62.5	500



Structures 1. Suggest your manuscript's ligand and Co (II) complex chemical structure.

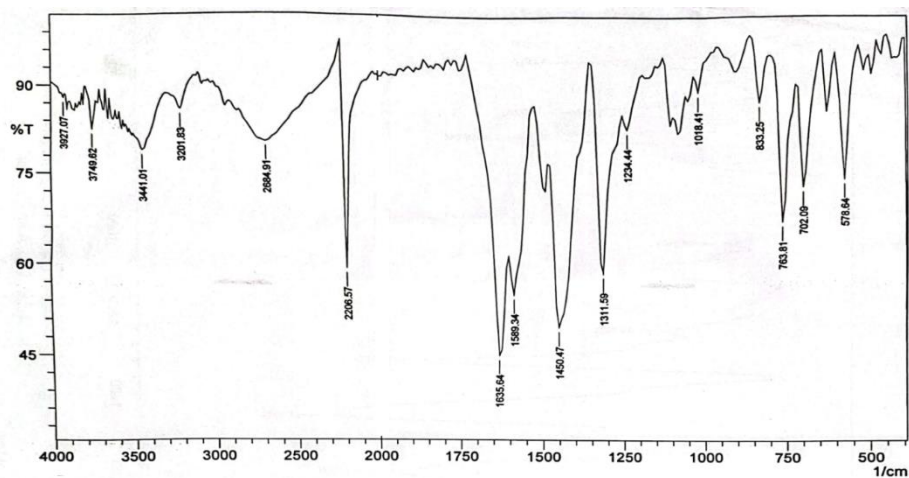


Figure1 FT-IR spectrum of ligand before irradiation

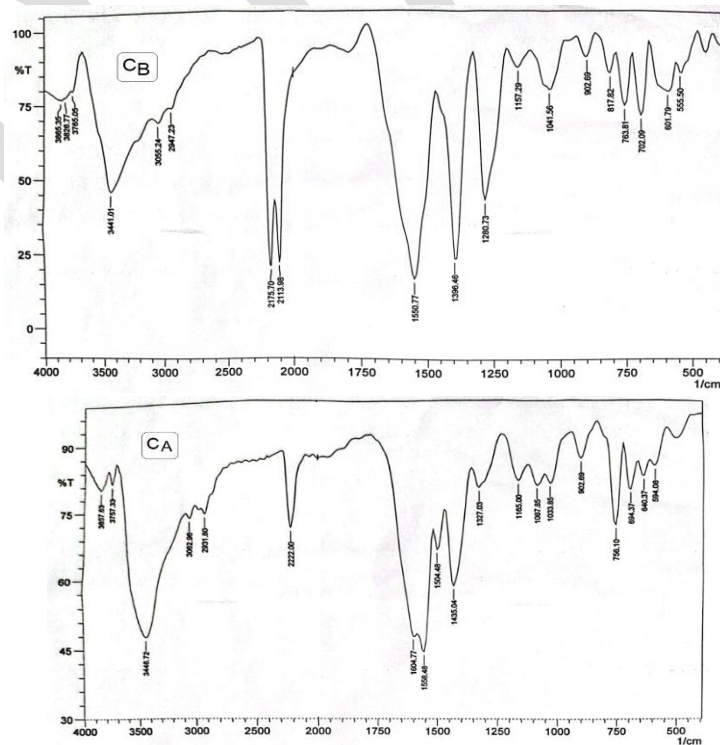


Figure2 FT-IR spectrum of Co (II) complexes before (C<sub>B</sub>) and after (C<sub>A</sub>) irradiation

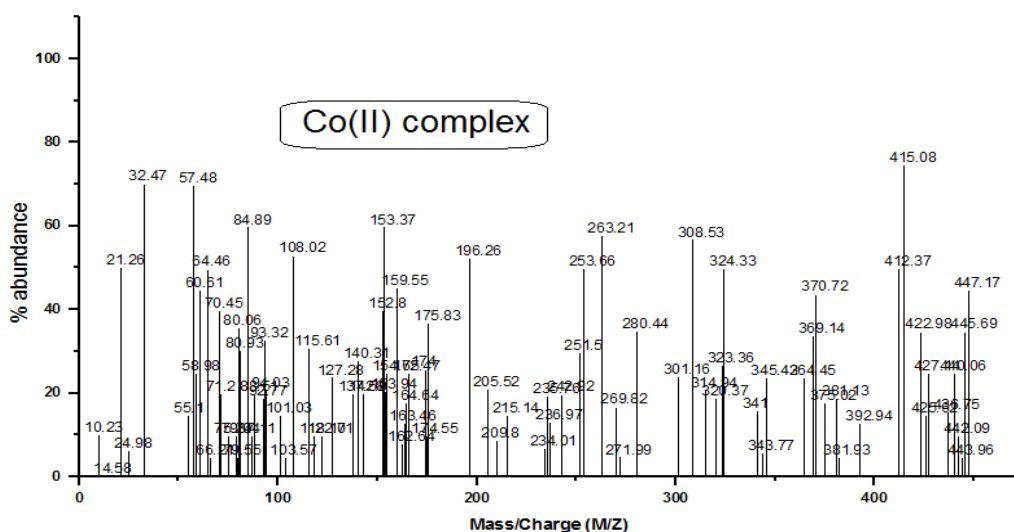


Figure 3. Mass spectra of ligand and Co (II) complexes

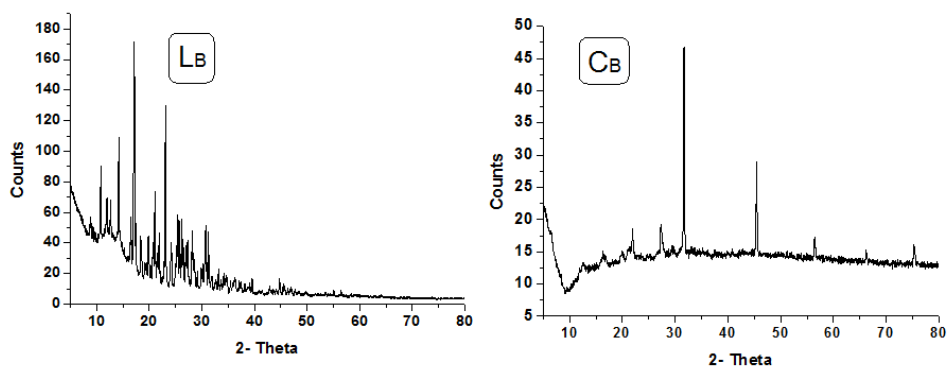


Figure 4. PXRD powder pattern of ligand and Co(II) complex.

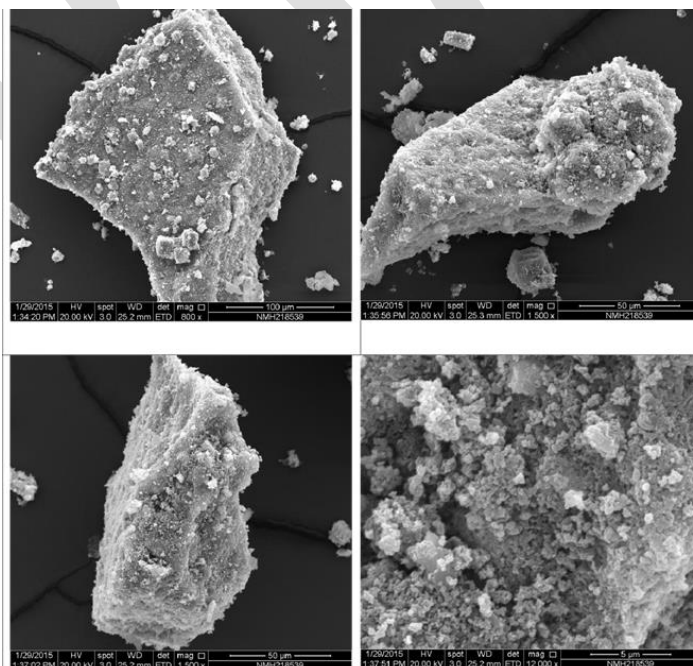
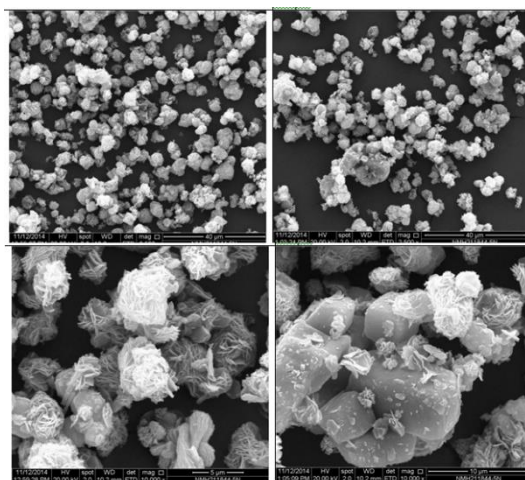
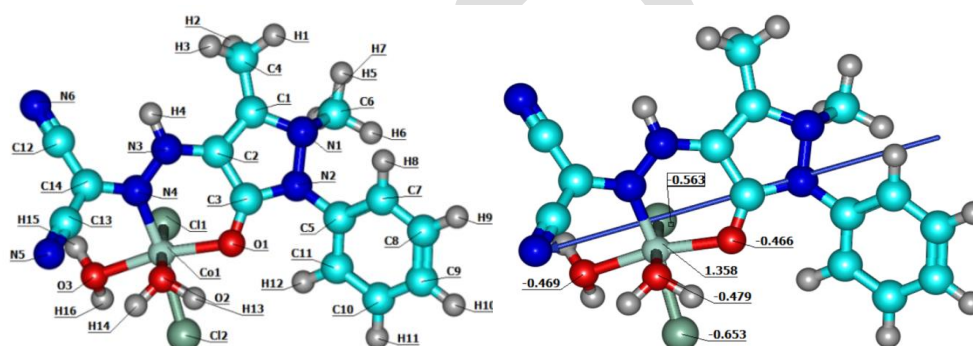


Figure 5. SEM of Co(II) complex before irradiation



**Figure 6.** SEM of Co(II) complex after irradiation



**Figure 7.** The optimized structure, the vector of the dipole moment, and the natural charges on active centers of  $[\text{CoLCl}_2(\text{H}_2\text{O})_2]$ .

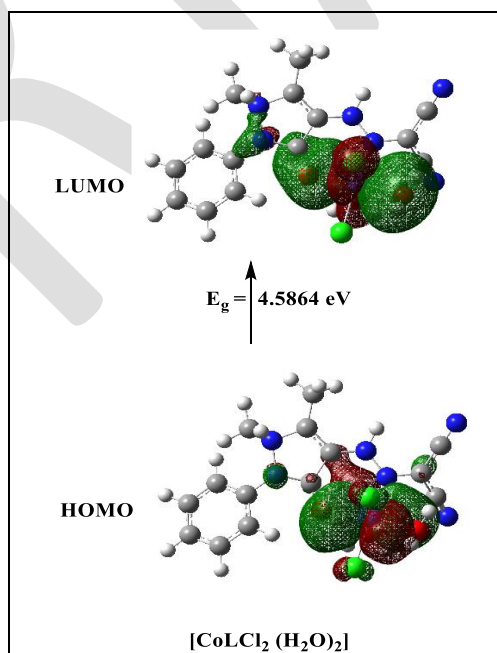


**Figure8:** MO and their energies of  $[\text{CoLCl}_2(\text{H}_2\text{O})_2]$

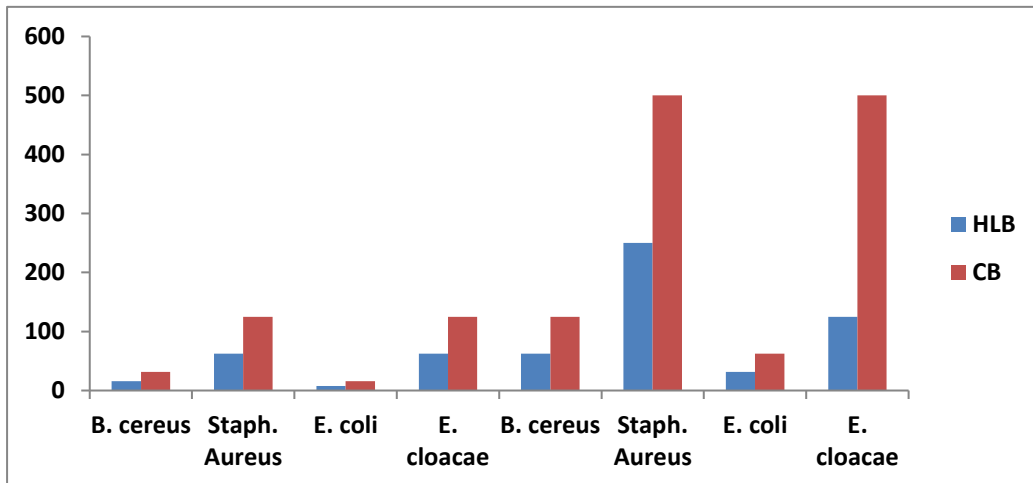


**Figure 9:** the antibacterial activity of Co(II) complex and ligand at a concentration of 10 mg ml<sup>-1</sup> in relation to gentamycin and ampicillin as standard medications

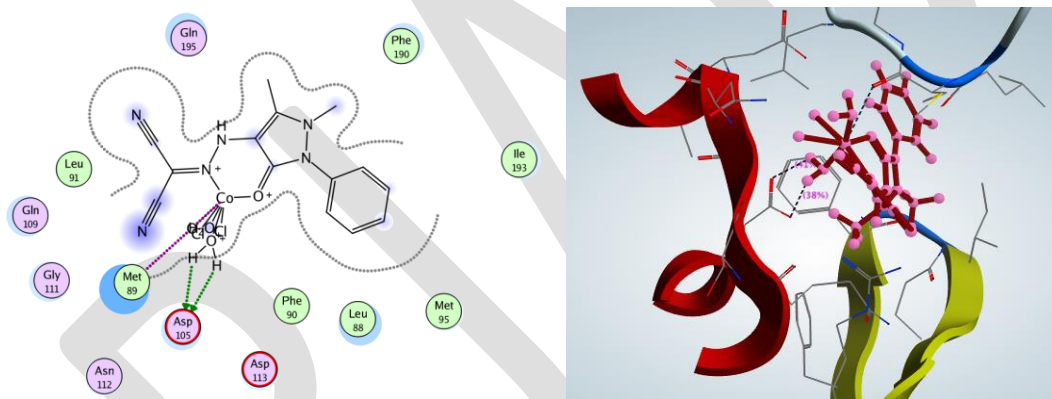


**Figure 10.** 2D and 3D Diagrams of the interaction between Co-complex and Penicillin-binding protein PBP enzyme.